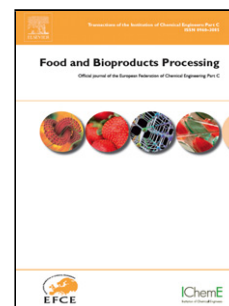


Accepted Manuscript

Title: Novel starch based nanocarrier for vitamin D fortification of milk: Production and characterization

Author: Elham Hasanvand Milad Fathi Alireza Bassiri Majid Javanmard Rouzbeh Abbaszadeh



PII: S0960-3085(15)00116-9
DOI: <http://dx.doi.org/doi:10.1016/j.fbp.2015.09.007>
Reference: FBP 648

To appear in: *Food and Bioproducts Processing*

Received date: 17-2-2015
Revised date: 30-5-2015
Accepted date: 14-9-2015

Please cite this article as: Hasanvand, E., Fathi, M., Bassiri, A., Javanmard, M., Abbaszadeh, R., Novel starch based nanocarrier for vitamin D fortification of milk: Production and characterization, *Food and Bioproducts Processing* (2015), <http://dx.doi.org/10.1016/j.fbp.2015.09.007>

This is a PDF file of an unedited manuscript that has been accepted for publication. As a service to our customers we are providing this early version of the manuscript. The manuscript will undergo copyediting, typesetting, and review of the resulting proof before it is published in its final form. Please note that during the production process errors may be discovered which could affect the content, and all legal disclaimers that apply to the journal pertain.

Novel starch based nanocarrier for vitamin D fortification of milk: Production and characterization

Elham Hasanvand¹; Milad Fathi^{2}; Alireza Bassiri³, Majid Javanmard¹, Rouzbeh Abbaszadeh¹*

¹*Department of Food Science and Technology, Institute of Agricultural Engineering, Iranian Research Organization for Science & Technology (IROST), Tehran, Iran*

²*Department of Food Science and Technology, Faculty of Agriculture, Isfahan University of Technology, Isfahan 84156-83111, Iran*

³*Department of Food Science and Technology, Institute of Chemical Engineering, Iranian Research Organization for Science & Technology (IROST), Tehran, Iran*

Abstract

Novel starch based nanoparticles were developed for entrapment of Vitamin D₃. High amylose starch nanocarriers had granular shape with particle size ranging from 14.2 to 31.8 nm with negative surface charge and narrow size distribution. VD₃ loaded nanocarriers had the encapsulation efficiency ranging from 37.06 to 78.11 %. The physicochemical properties of nanocarriers were characterized by Fourier transform-infrared spectroscopy, X-ray diffraction and differential scanning calorimetry and indicated well entrapment of encapsulant. Release behavior of vitamin D₃ was studied in gastro-intestinal media and Rigter-Peppas and wibull models were the most suitable for describing the entire release behavior. Release phenomenon is mostly governed by of Fickian mechanism. The potential ability of nanocarriers for food fortification was studied using milk as a calcium rich model food. Sensory analysis performed for fortified milk and results implicated that the developed nanocarriers did not show any significant difference with blank milk sample and could well mask the after taste and eliminate poor solubility of vitamin D₃. The results illustrated that nanoparticles can be used for the fortification of food to improve bioavailability of vitamin D₃ or other hydrophobic compounds.

Keywords: Vitamin D₃; Starch nanocarriers; Controlled release.

1. Introduction

Functional foods provide addition functions to ensure or enhance public health. They could be produced by fortification applying bioactives such as vitamins and antioxidants. However, the bioavailability of bioactives ingredients decrease during processing, storage or consumption due to their sensitivity and low aqueous solubility

* . Corresponding author: Tel.: +98 31 33913368; Fax: +98 31 33913381. e-mail: mfathi@cc.iut.ac.ir

(Barrow et al., 2009; Cohen et al., 2008; Madrigal-Carballo et al., 2010; Rajam et al., 2012; Shimoni and Gustavo, 2009; Teng et al., 2013b). Nanoencapsulation which is entrapment of bioactive within a nanoscale carrier is an appropriate technology to overcome these limitations. This technique increases bioactive solubility, enhance release behavior, cellular uptake and bioavailability (Chen et al., 2006; Ezhilarasi et al., 2013; Fathi et al., 2014; Mozafari et al., 2008). Selection of appropriate shell and method for nanoencapsulation is an important and interesting field of research. The applied shell for entrapment of food bioactive should meet some criteria such as biocompatibility and biodegradability. The applied production method also should be appropriate for large scale production (Matalanis et al., 2011). Starch which found abundantly in nature, is a good candidate for production of nano-delivery systems. It also causes slow release, inhibition of inadvertent release, reducing probable complications due to overdose and more effectiveness of sensitive ingredients (Kreuter, 2007; Simi and Abraham, 2007; Singh and Lillard Jr, 2009). Starch structure is known as “double helix” (Hancock and Tarbet, 2000) that consists of two types of molecules: the linear and helical amylose and the branched amylopectin (Davis et al., 2003). The natural and spontaneous tendency of amylose to form single helical molecular inclusion complexes, termed V amylose (Biliaderis and Galloway, 1989; Eliasson and Krog, 1985; Raphaelides and Karkalas, 1988; Tufvesson et al., 2003a, b). It has a central hydrophobic cavity interconnected by amorphous regions of the polysaccharide chains which render the complexes fairly stable to acidic hydrolysis and may be used as a possible platform for the encapsulation of hydrophobic molecules (Biais et al., 2006; Biliaderis, 1998; Cui, 2005; Heinemann et al., 2003; Heinemann et al., 2005; Kawada and Marchessault, 2004; Le Bail et al., 2005). So far starch nanoparticles have been used as carrier of flax seed oil, (Gökmen et al., 2011) unsaturated fatty acids, (Lesmes et al., 2009; Zabar et al., 2009) and flavors (Heinemann et al., 2003; Itthisoponkul et al., 2007). Six main methods have been reported for production of biopolymer nanoparticles :i) Nanoprecipitation, ii) Emulsion–diffusion, iii) Double emulsification, iv) Emulsion-coacervation, v) Polymer-coating, vi) Layer-by-layer (Mora-Huertas et al., 2010).

All of these methods usually are applied in the two ways: i) the solvent free that the dried amphiphilic polymer is dissolved in water and after hydrating, they are shaped like vesicles ii) displacement techniques which copolymer is dissolved in an organic solution and water is added then the organic solution subsequently being removed. In order to reach mono size distributions of the polymer vesicles, the obtained suspension can be treated by sonication, vortexing, extrusion and freeze-thaw cycles or combination of these techniques (Kita-Tokarczyk et al., 2005).

Sonication is widely used due to saving energy, reduction of process time and increase of encapsulation efficiency (Jambrak et al., 2009; Mason et al., 1996). Ultrasonic cavitation phenomenon includes forming, developing and bursting of micro-bubbles in solutions that causes production of large amounts of energy, high temperature and high pressure in solution which leads to destruct bonds between molecular of biopolymers (Kawasaki et al., 2007; Tischer et al., 2010).

Vitamin D is a fat-soluble bioactive, which is sensitive to light, heat and oxygen (Ballard et al., 2007). It is used in mineral metabolism especially associated with calcium and phosphorus and prevents diabetes mellitus, hypertension and multiple sclerosis (MS) (El-Hajj Fuleihan and Vieth, 2007; Pettifor and Prentice, 2011; Picciano, 2010; Pittas et al., 2010). Vitamin D is synthesized either in skin by sunlight or provided by the food (Hickey and Gordon, 2004). Food sources of vitamin D is very limited and its deficiency in many countries has been reported (Gessner et al., 2003; Rucker et al., 2002).

In this study high amylose corn starch nanoparticles were developed for the first time using ultrasonication to encapsulate vitamin D and their physicochemical and release behavior were studied. The potential application of nanocarriers for fortification of milk was investigated.

2. Materials and methods

2.1. Materials

High amylose corn starch (HACS) with 70% Amylose was purchased from Sigma–Aldrich (St. Louis, MO, USA). Vitamin D₃ was supplied from DSM (Roche) company (Village -Neuf, France) and alpha-amylase (Termamyl®) was obtained from Novozymes A/S (Denmark). Potassium hydroxide, n-Hexan and all other chemicals were of analytical grade and obtained from Merck (Darmstadt, Germany). Double distilled water used in this study.

2.2. Production of nanoencapsulated vitamin D₃

HACS solution in 0.1 M KOH (w/v) preheated at 80°C ± 1 °C for 30 min and cooled to 30 °C ± 1 °C. VD₃ solution in

pure ethanol was added dropwise into starch solution with mild stirring for 1 min (Lesmes et al., 2008). The alkali

mixture was subjected to a 24 Kz probe-type ultrasound (Misonix, S-4000, USA). The sample was exposed to 60 cycles of sonication for 10 seconds, after each cycle, sonication for 10 seconds stops which allows the sample to cool in a cold water bath. The obtained suspension was frozen at -18 °C, dried using freeze-dryer (Christ α 1-4 model, Germany) and grinded into fine powder. Table 1 shows the formulation of different nanocarriers.

2.3. Determination of encapsulation efficiency (EE) and loading efficiency (LE)

Ten milligrams of the freeze-dried nanoparticles was washed with 5 mL hexane and the suspension was filtrated through a Whatman No. 1 filter paper. The filtrate was subjected to spectrophotometric measurement at 264 nm with a LAMBDA 25 UV/VIS spectrophotometer (Perkin Elmer, Waltham, Massachusetts). This procedure was repeated until the absorption of last filtrate became insignificant. Then all the filtrates were combined and measured again for its absorbance at 264 nm, which showed the amount of free VD₃. The nanoparticles remained after the filtration was dried and weighed. The EE and LE of the samples were calculated with the equation:

$$EE(\%) = 100 - \left(\frac{\text{Weight of free vitamin D}}{\text{Weight of initial vitamin D used}} \times 100 \right) \quad (1)$$

$$LE(\%) = \frac{\text{Weight of vitamin D loaded in nanoparticles}}{\text{Weight of nanoparticles}} \times 100 \quad (2)$$

2.4. Particle size, polydispersity index and zeta potential

The average particle size, polydispersity index (PDI) and zeta potential of nanoparticle of vitamin D carrier were determined by a dynamic light scattering (DLS) (90Plus Nanoparticle Size Analyzer, Brookhaven Instruments).

2.5. Morphology characterization

The morphology of VD-loaded nanoparticles was observed by scanning electron microscopy (MIRA-FEG, TESCAN, Czech Republic). Drib of the nanoparticle dispersions was dripped and cast-dried on an aluminium pan, which was cut into appropriate sizes. The samples were then coated with a thin layer (<20 nm) of gold using a sputter coater (Hummer XP, Anatech, CA, USA).

2.6. Vitamin D₃ release and modeling

Dialysis bag method was used to assess release behavior of the nanocarriers. Five milliliters of vitamin D₃ loaded nanocarrier solution was sealed into dialysis bag (Sigma, Canada) with a 12-kDa cutoff at 37 °C and 100 rpm. The bag was then put into 35 ml gastric buffer (PH =1.2) for 2 h. It was subjected to enzymatic digestion by pancreatic amylases in intestinal buffer (35 ml, pH = 7.4) containing alpha-amylase for 6 h. Gastric media with pH of 1.2 consisted of KCl (2.0 g) and HCl (7 mL) and intestinal media with pH 7.4 prepared by KH₂PO₄, and NaOH (Jain et

al., 2007). At specified time intervals (for gastric buffer every 20 minutes and for intestinal buffer every 60 minutes), 3 ml of buffer was removed and freeze dried whereas the same volume of fresh media was added to maintain a constant volume. The powder yielded after lyophilization was suspended in cold hexane and extracted under vigorous stirring for 1 min. The suspension was then filtered and measured for its absorbance at 264 nm with UV/VIS spectrophotometer (Li et al., 2014a; Teng et al., 2013a).

The vitamin D₃ release data were kinetically evaluated by 8 models (Zero order, First order, Higuchi, Korsmeyer-Peppas, Baker-Lonsdale, Weibull, Quadratic, and Hixson-Crowen) (Costa and Sousa Lobo, 2001; Dash et al., 2010; Singhvi and Singh, 2011) (Eqs. 3–10):

$$C = Kt \quad (3)$$

$$\ln C = Kt \quad (4)$$

$$C = Kt^{0.5} \quad (5)$$

$$C = Kt^n \quad (6)$$

$$\frac{3}{2} [1 - (-C)^{2/3}] - C = Kt \quad (7)$$

$$\log(-\ln(1 - C)) = b \times \log t - \log a \quad (8)$$

$$C = 100 (K_1 t^2 + K_2 t) \quad (9)$$

$$-C^{\frac{1}{3}} = Kt \quad (10)$$

where C is vitamin D₃ concentration (%) at time t , K is kinetic constant, and n is release exponent. The latest is used to characterize different release mechanisms. Encapsulant release from spherical carriers with $0.43 > n$ is controlled by Fickian diffusion mechanism, and $n \geq 0.85$ is commanded for dissolution phenomenon, and $0.43 < n \leq 0.85$ is governed by combination of two mechanisms (Siepmann et al., 2012; Tiwari and Tiwari, 2013). The shape parameter, in Weibull model characterizes the curve as either exponential, ($b = 1$) (Case 1), sigmoid, S-shaped, with upward curvature followed by a turning point ($b > 1$) (Case 2), or parabolic, with a higher initial slope and after that consistent with the exponential ($b < 1$) (Case 3) (Costa and Sousa Lobo, 2001).

2.7. Thermal analysis

Thermal transition properties of pure materials, physical mixture of starch and vitamin D₃ with weight ratio similar to formulations and VD₃ loaded nanocarriers were examined using a differential scanning calorimeter (DSC -60,

Shimadzu, Tokyo, Japan). The instrument was calibrated with indium and an empty pan was used as the reference. Two milligrams sample was added to 6.0 μ l of distilled water and sealed in aluminum DSC pans. After equilibration overnight, the solution was scanned from 0 to 330 °C in the calorimeter at 10 °C/min.

2.8. X-ray diffraction analysis

The crystallographic structural analysis was carried out by X-ray diffractometer (XRD- EQUINOX 3000, INEL, France). The operating conditions were Cu K-alpha-1 radiation (0.154 nm), voltage 40 kV and current 30 mA. Approximately 200 mg of sample powders were loaded onto an aluminum plate and scanned over the range -10–118 Bragg angles in steps of 0.02° per second.

2.9. Fourier transform infrared spectroscopy

Fourier-transform infrared spectroscopic studies were performed in transmission mode using Philips PU9624 FTIR spectrometer. The FTIR spectra of pure materials and physical mixture were compared with VD₃ loaded nanoparticle. Tablets comprising of 300 mg of KBr and 2 mg of samples were prepared for FTIR tests. Spectra were obtained at 4 cm⁻¹ of resolution from 4000 cm⁻¹ to 400 cm⁻¹ (Li et al., 2014b; Shi et al., 2012; Tay et al., 2012).

2.10. Sensory properties

Due to high consumption of milk in human diet and excellent source of calcium, it was selected as a sample food system to develop potential functional food enriched with VD₃ loaded nanoparticle. Three milk samples, i.e., blank (2.5 % fat sterilized milk; Pegah Company), VD₃ loaded nanocarrier fortified milk (0.16 %, w/v) and direct VD₃ fortified milk (at the same concentration contained in nanocarriers), were presented at temperature about 14 ± 2 °C and assessed using hedonic scale of 1–7. Eight expert panelists evaluated the sensory properties of the fortified milk samples using palatal and non-palatal properties. The attributes divided into groups of color, homogeneity, taste (creaminess, sweetness, bitter taste and after taste) and total acceptance (Chojnicka-Paszun et al., 2012; Fathi et al., 2013).

2.11. Statistical analysis

All experiments were performed at least in three replications, and average values were reported. Statistical analyses were carried out using SPSS 16 software. Data were subjected to analysis of variance, and means were compared using “Duncan” test at 5% significant level.

3. Results and Discussion

3.1. Particle size, zeta potential, encapsulation efficiency, and encapsulation load

Vitamin D₃ loaded nanoparticles were produced using high power ultrasonic method, based on use of various concentrations of soluble starch (2 and 4%), vitamin D₃ concentrations in emulsion (1.25 and 2.5%) and ultrasonic powers (300 and 450 W). Table 2 shows size, PDI, zeta potential, encapsulation efficiency, and encapsulation load of nanoparticles. According to the Table 2, all the samples had almost the same sizes (less than 40 nm) and there was no significant difference ($p < 0.05$) between treatments. Enhancement of absorption is the preliminary mean for increasing the bioavailability of a poorly water soluble compounds (Hörter and Dressman, 2001). Since the bioavailability of a poorly water soluble compound is dissolution rate limit, use of nanometer sized particles by enhancing dissolution rate improves bioavailability especially for compounds that are adsorbed at a defined region of the gastrointestinal tract (Jinno et al., 2006; Kocbek et al., 2006; Merisko-Liversidge and Liversidge, 2008). Smaller the particle size the higher the stability against the gravity due to Brownian motion (Mason et al., 2006). All samples have PDI value less than 0.4 which is an indicative of their narrow size distribution. Zeta potential values of all samples were negative. The maximum absolute value of the zeta potential was related to the formulation No. 2. High absolute values of zeta potential led to higher repulsion force of particles and emulsion stability (Üner, 2006). All three factors and their interactions had significant effect ($p < 0.05$) on the zeta potential.

The results indicated that for most of treatment increasing vitamin concentration leads to higher encapsulation efficiency. The interaction of starch concentration and vitamin D probably related to formation of hydrogen bonds between vitamin D and starch that caused a decrease in the negative surface charge (see FTIR results). For example, the formulation No 8 showed, EE value higher than 71% which showed numerous interactions between vitamin D and starch while had the least zeta potential in contrast to formulation No. 2. Statistical analysis revealed that the LE significantly enhanced ($p < 0.05$) with increasing ultrasonic power and vitamin D₃ concentration. Similar results were obtained by Chin et al (2014). Interaction of starch-vitamin has significant effect ($p < 0.05$) on load efficiency. Formulation No. 8 possessed the highest LE, which based on to XRD results, could be related to formation of a V-type structure and creation of a hydrophobic helix where is capable of accepting more vitamin D. Samples had lower levels of LE (No. 1, 5 and 7) possessed high release rate. While for formulation No. 6 and 8 with higher LE the slow release is observed, which is due to formation of hydrogen bonds between vitamin D and starch and change of glycosidic bonds of starch that reduces the effect of alpha-amylase.

3.2. Morphology

SEM images showed nanoparticles had granular morphology with size range of 30 to 40 nm. These observations are in agreement with the DLS data. It seems that nanoparticles that synthesized with 2% concentration of starch (Fig.1 a, b, c, and d) are less aggregated than those with 4% concentration of starch (Fig.1 e, f, g, and h) which could be attributed to their higher surface charge that are in agreement with zeta potential data. The ultrasonication via degradation of starch molecules leads to formation of nanoparticles, which shows some disarrays in the surface. Furthermore, it can be seen that the granules were exposed to sonication under 450 W power are clustered (Fig .1 c, d, g, and h). Amylose molecules would be agglomerated during processing and the laceration of hydrogen bonds, provided favorable conditions for novel connections and links between the polymers (Jambrak et al., 2010). Disruption of the starch chains could be induced by increasing the severity of ultrasound application (Gonçalves et al., 2014) .

3.3. Vitamin D₃ release and modeling

Figure 2 shows the release profile of vitamin D₃ loaded starch nanoparticle. The release rate in first 2 h (gastric condition) in all formulations was found to be less than 3.5%. During the next 8 hours, high amount of vitamin D released in simulated intestinal solution in the presence of alpha-amylase. These results strongly indicated that starch nanoparticles are good candidate for protecting encapsulated agents against acidic and enzymatic conditions of stomach and increasing their absorption and bioavailability. This is an opportunity to absorb more vitamin D for oral delivery through fortified foods. All of nanoparticle showed a primary burst release under intestinal conditions, afterward vitamin D started to gradual release. The highest rate of digestion of nanocarriers is related to 20-120 minutes of initial time in small intestine (Englyst et al., 1992; Lehmann and Robin, 2007). It is noteworthy that due to using fairly high temperature during production the digestion of starch increased in comparison to intact high amylose starch. The small size of the particles allows enzyme access to substance and particle degradation (Jain et al., 2008).

The maximum releases of formulations 1, 3, 5 and 7 after 8 hours were much greater than formulations of 2, 6 and 8. It could be due to glycosidic bonds (see FTIR results), then treating with ultrasonic and finally breaking of these bonds by α -amylase which led to faster release of Vitamin D. Modeling results for eight different kinetic models are tabulated in Table 3. The poor ability of zero-order model specified that release mechanism depends on

concentration. The n values of the Rigter-Peppas model were lower than 0.43 informing that the release is governed by the Fickian mechanism. For the most formulations the b values of Weibull model were lower than 1 indicated a parabolic release curve with a higher initial slope and then a consistent exponential release. These results showed that although there is an initial burst release, but release of vitamin D continued with almost constant velocity. Rigter-Peppas and Weibull models showed highest correlation coefficient and had better ability to describe release behavior of vitamin D from starch nanoparticle.

.3.4 Fourier transform infrared spectroscopy

FTIR spectra (Figure 3) showed strong adsorption peaks for pure high amylose starch at 3434 cm^{-1} , which is attributed to the O-H stretching of starch and its breadth indicated the extent of formation of inter- and intramolecular hydrogen bonds. The unsymmetrical stretching of C-H (CH_2 group) is observed at 2927 cm^{-1} and the absorption band at 1643 cm^{-1} is due to the presence of bounded water in starch (Simi and Abraham, 2007; van Soest et al., 1995). Other peaks, at 1160 cm^{-1} and 1082 cm^{-1} are associated with C-O bond and C-C bond, which were visible in physical mixture spectra while they are much weaker for nanoparticle. The peak at 1371 cm^{-1} represents the angular deformation of C-H (CH_3 group). Similarly the peak at 987 cm^{-1} related to the C-O-C of α -1,4 and α -1,6 glycosidic linkages (Shi et al., 2012). Some bands were observed on the spectrogram of VD_3 , for hydrogen bonded O-H stretch (3292 cm^{-1}), alkyl C-H stretch (2935 and 2874 cm^{-1}) and several others indicating C-H bend in the range of 1052 – 1451 cm^{-1} . Regarding the mixture of starch and vitamin D, the major absorption peaks of vitamin D and starch were still observed. However, the skeletal vibration of vitamin D disappeared for the prepared vitamin D encapsulated starch (the lesser band at proximity 2950 and 1000 – 1700 in the spectrum loaded vitamin D nanoparticle was derived from starch). This indicated that the vitamin D is incorporated into the helix of amylose. An interesting characterization peak was in the range of 3400 – 3550 cm^{-1} , indicating the hydrogen bonds. It is suggested that the hydrogen bonds were formed between VD_3 and high amylose starch. Therefore, it was considered as one of the main forces facilitating nanoparticle formation.

.3.5 X-ray diffraction analysis

XRD patterns of high amylose corn starch peaks appeared at 17.12 , 16.27 , 22.2 (2θ) which were characterized as B-type crystals (Kim et al., 2012). For pure vitamin D two intense peaks, detected at angles (2θ) 16.93 and 17.3 . Figure 4 shows that the XRD of the physical mixtures had intensity peaks highly similar to those of pure vitamin D

crystals, as can be seen well in the range of 16.62-17.3 of Bragg angles [2 θ]. This shows that intensity peaks, arising from vitamin D crystals, considerably include those of relatively amorphous starch.

Diffraction peaks of starch and the physical mixtures were disappeared, indicating a substantial disruption of the crystalline structure by the ultrasonic treatment. Compared to HACS, all the diffraction peaks of the nanoparticles exhibited a broad peak from 5° to almost 27° (except formulations 8) associated with an amorphous phase. On the other hand, vitamin D intense peaks were removed which suggested that it was successfully encapsulated in the starch. XRD obtained for nanocarrier of formulation 8 have a rather violent peak at Bragg angle 20, that demonstrate similarity to previously recorded XRDs of V-amylose structures. Formation of a V-type complex was verified by measuring the X-ray diffraction of starch- included complexes in previous studies (Lalush et al., 2005; Le Bail et al., 2005; Lesmes et al., 2008). Moreover in other nanocarriers peaks appeared at Bragg angle 27 and 39.5, which indicating formation of a new crystalline form of encapsulation of vitamin D in starch. However, it can be mentioned that the crystallinity of the nanoparticles is less than starch and physical mixture. It was assumed that the ultrasonic treatment led to changes in the structure of the starch granules, especially the crystalline regions of amylopectin (Bel Haaj et al., 2013; Sun et al., 2014; Zhu et al., 2012). On the other hand the results of DLS and SEM confirmed that the particle size is small and since the width at the half height of a peak is inversely proportional to the particle size therefore with decreasing particle size the diffraction peak became broader (Bel Haaj et al., 2013).

.3.6 Thermal properties

The DSC thermograms corresponding to HACS, VD₃, physical mixture and vitamin D loaded nanoparticles are shown in Figure 5. Vitamin D₃ exhibited sharp peak at 87.8 °C indicating its melting point and its crystal structure.

Achange in slope at outskirts 60 °C in inverse DSC thermogram of HACS could be observed, corresponding to the

glass transition point and indicating of starch amorphous structure. Endothermic peak at 286 °C is the result of

decomposition of starch. It is in agreement with previous study reported by Tian et al (2013). All the physical mixtures showed endothermic peaks at 87 and 286 °C that corresponded to the melting of vitamin D and depolymerization of starch. Vitamin peak did not observe in the thermograms of nanoparticles, showing appropriate encapsulating of vitamin. Also a change of slope at 80 °C and crystallization temperature at 210-220 °C for nanoparticle, implied an increase in the glass transition temperature and crystallinity of nanoparticle in comparison to pure starch. Encapsulation of vitamin D in starch will increase its thermal resistance against heat processing. XRD data also approved that semi-crystalline structure is created in the nanocarriers.

3.7. Sensory analysis

To evaluate the ability of nanoparticles for food enrichment, the lyophilized nanocarriers were added to milk sample as a food system with high calcium content. The sensory results of blank, fortified milk with VD₃ loaded nanocarriers and with direct VD₃ addition were depicted in Fig. 6. Scores assigned for vitamin D₃ fortification identified that direct adding vitamin D₃ led to significant ($p < 0.05$) increase in after taste and decrease in degree of homogeneity and total acceptance. Low homogeneity concerned that vitamin D is much less soluble in aqueous medium and makes grittiness mode in texture of milk. On the other hand, sensory properties of fortified milk with nanoparticles of vitamin D were quite similar to blank milk sample. Due to the small size of nanoparticles they can be used as delivery systems in order to enhance the stability of the emulsion and improve the taste of fortified food.

4. Conclusion

We have successfully loaded vitamin D₃ into starch nanoparticles under a low term process using ultrasonic method and their features were investigated. Carriers had sizes under nano range with negative zeta potential. XRD analysis showed that the crystallinity of produced nanocarriers were less than pure materials and indicated that the vitamin D₃ was successfully entrapped in starch. DSC thermogram confirmed that encapsulation in starch protect VD₃ against thermal degradation. Hydrogen bond was considered to be the major force facilitating the formation of nanoparticles based on FTIR data. In vitro release behavior of VD₃ in gastric condition was very low while a rapid initial released observed in intestinal media. Kinetic study in gastrointestinal conditions revealed that Rigter-Peppas and Wibull were the best models for describing vitamin D₃ release. The results of sensory analysis showed that nanoencapsulation could improve the taste, homogeneity, and total acceptance of fortified milk. Thus starch nanoparticles are promising carriers for VD₃ and other hydrophobic food bioactives.

5. References

- Ballard, J.M., Zhu, L., Nelson, E.D., Seburg, R.A., 2007. Degradation of vitamin D₃ in a stressed formulation: The identification of esters of vitamin D₃ formed by a transesterification with triglycerides. *Journal of pharmaceutical and biomedical analysis* 43, 142-150.
- Barrow, C.J., Nolan, C., Holub, B.J., 2009. Bioequivalence of encapsulated and microencapsulated fish-oil supplementation. *Journal of functional foods* 1, 38-43.
- Bel Haaj, S., Magnin, A., Pétrier, C., Boufi, S., 2013. Starch nanoparticles formation via high power ultrasonication. *Carbohydrate polymers* 92, 1625-1632.
- Biais, B., Le Bail, P., Robert, P., Pontoire, B., Buleon, A., 2006. Structural and stoichiometric studies of complexes between aroma compounds and amylose. Polymorphic transitions and quantification in amorphous and crystalline areas. *Carbohydrate Polymers* 66, 306-315.
- Biliaderis, C., 1998. Structures and phase transitions of starch polymers. *ChemInform* 29.
- Biliaderis, C.G., Galloway, G., 1989. Crystallization behavior of amylose-V complexes: structure-property relationships. *Carbohydrate Research* 189, 31-48.
- Chen, L., Remondetto, G.E., Subirade, M., 2006. Food protein-based materials as nutraceutical delivery systems. *Trends in Food Science & Technology* 17, 272-283.
- Chojnicka-Paszun, A., De Jongh, H., De Kruif, C., 2012. Sensory perception and lubrication properties of milk: Influence of fat content. *International Dairy Journal* 26, 15-22.
- Cohen, R., Orlova, Y., Kovalev, M., Ungar, Y., Shimoni, E., 2008. Structural and functional properties of amylose complexes with genistein. *Journal of agricultural and food chemistry* 56, 4212-4218.
- Costa, P., Sousa Lobo, J.M., 2001. Modeling and comparison of dissolution profiles. *European journal of pharmaceutical sciences* 13, 123-133.
- Cui, S.W., 2005. *Food carbohydrates: chemistry, physical properties, and applications*. CRC Press.
- Dash, S., Murthy, P.N., Nath, L., Chowdhury, P., 2010. Kinetic modeling on drug release from controlled drug delivery systems. *Acta Pol Pharm* 67, 217-223.

Davis, J.P., Supatcharee, N., Khandelwal, R.L., Chibbar, R.N., 2003. Synthesis of novel starches in planta:

opportunities and challenges. *Starch-Stärke* 55, 107-120.

El-Hajj Fuleihan, G., Vieth, R., 2007. Vitamin D insufficiency and musculoskeletal health in children and adolescents. *International Congress Series* 1297, 91-108.

Eliasson, A.-C., Krog, N., 1985. Physical properties of amylose-monoglyceride complexes. *Journal of Cereal Science* 3, 239-248.

Englyst, H.N., Kingman, S., Cummings, J., 1992. Classification and measurement of nutritionally important starch fractions. *European journal of clinical nutrition* 46, S33-50.

Ezhilarasi, P., Karthik, P., Chhanwal, N., Anandharamakrishnan, C., 2013. Nanoencapsulation techniques for food bioactive components: a review. *Food and Bioprocess Technology* 6, 628-647.

Fathi, M., Martín, Á., McClements, D.J., 2014. Nanoencapsulation of food ingredients using carbohydrate based delivery systems. *Trends in Food Science & Technology* 39, 18-39.

Fathi, M., Varshosaz, J., Mohebbi, M., Shahidi, F., 2013. Hesperetin-loaded solid lipid nanoparticles and nanostructure lipid carriers for food fortification: preparation, characterization, and modeling. *Food and Bioprocess Technology* 6, 1464-1475.

Gessner, B.D., Plotnik, J., Muth, P.T., 2003. 25-Hydroxyvitamin D levels among healthy children in Alaska. *The Journal of pediatrics* 143, 434-437.

Gökmen, V., Mogol, B.A., Lumaga, R.B., Fogliano, V., Kaplun, Z., Shimoni, E., 2011. Development of functional bread containing nanoencapsulated omega-3 fatty acids. *Journal of Food Engineering* 105, 585-591.

Gonçalves, P.M., Noreña, C.P.Z., da Silveira, N.P., Brandelli, A., 2014. Characterization of starch nanoparticles obtained from *Araucaria angustifolia* seeds by acid hydrolysis and ultrasound. *LWT-Food Science and Technology* 58, 21-27.

Hancock, R.D., Tarbet, B.J., 2000. The other double helix—the fascinating chemistry of starch. *Journal of Chemical Education* 77, 988.

- Heinemann, C., Escher, F., Conde-Petit, B., 2003. Structural features of starch–lactone inclusion complexes in aqueous potato starch dispersions: the role of amylose and amylopectin. *Carbohydrate polymers* 51, 159-168.
- Heinemann, C., Zinsli, M., Renggli, A., Escher, F., Conde-Petit, B., 2005. Influence of amylose-flavor complexation on build-up and breakdown of starch structures in aqueous food model systems. *LWT-Food Science and Technology* 38, 885-894.
- Hickey, L., Gordon, C.M., 2004. Vitamin D deficiency: new perspectives on an old disease. *Current Opinion in Endocrinology, Diabetes and Obesity* 11, 18-25.
- Hörter, D., Dressman, J., 2001. Influence of physicochemical properties on dissolution of drugs in the gastrointestinal tract. *Advanced drug delivery reviews* 46, 75-87.
- Itthisoponkul, T., Mitchell, J.R., Taylor, A.J., Farhat, I.A., 2007. Inclusion complexes of tapioca starch with flavour compounds. *Carbohydrate polymers* 69, 106-115.
- Jain, A.K., Khar, R.K., Ahmed, F.J., Diwan, P.V., 2008. Effective insulin delivery using starch nanoparticles as a potential trans-nasal mucoadhesive carrier. *European Journal of Pharmaceutics and Biopharmaceutics* 69, 426-435.
- Jain, S.K., Jain, A., Gupta, Y., Ahirwar, M., 2007. Design and development of hydrogel beads for targeted drug delivery to the colon. *AAPS PharmSciTech* 8, E34-E41.
- Jambrak, A.R., Herceg, Z., Šubarić, D., Babić, J., Brnčić, M., Brnčić, S.R., Bosiljkov, T., Čvek, D., Tripalo, B., Gelo, J., 2010. Ultrasound effect on physical properties of corn starch. *Carbohydrate Polymers* 79, 91-100.
- Jambrak, A.R., Lelas, V., Mason, T.J., Krešić, G., Badanjak, M., 2009. Physical properties of ultrasound treated soy proteins. *Journal of Food Engineering* 93, 386-393.
- Jinno, J.-i., Kamada, N., Miyake, M., Yamada, K., Mukai, T., Odomi, M., Toguchi, H., Liversidge, G.G., Higaki, K., Kimura, T., 2006. Effect of particle size reduction on dissolution and oral absorption of a poorly water-soluble drug, cilostazol, in beagle dogs. *Journal of controlled release* 111, 56-64.

Kawada, J., Marchessault, R.H., 2004. Solid State NMR and X-ray Studies on Amylose Complexes with Small

Organic Molecules. *Starch-Stärke* 56, 13-19.

Kawasaki, H., Takeda, Y., Arakawa, R., 2007. Mass spectrometric analysis for high molecular weight synthetic polymers using ultrasonic degradation and the mechanism of degradation. *Analytical chemistry* 79, 4182-4187.

Kim, H.Y., Lee, J.H., Kim, J.Y., Lim, W.J., Lim, S.T., 2012. Characterization of nanoparticles prepared by acid hydrolysis of various starches. *Starch-Stärke* 64, 367-373.

Kita-Tokarczyk, K., Grumelard, J., Haeefe, T., Meier, W., 2005. Block copolymer vesicles—using concepts from polymer chemistry to mimic biomembranes. *Polymer* 46, 3540-3563.

Kocbek, P., Baumgartner, S., Kristl, J., 2006. Preparation and evaluation of nanosuspensions for enhancing the dissolution of poorly soluble drugs. *International journal of pharmaceutics* 312, 179-186.

Kreuter, J., 2007. Nanoparticles—a historical perspective. *International Journal of Pharmaceutics* 331, 1-10.

Lalush, I., Bar, H., Zakaria, I., Eichler, S., Shimoni, E., 2005. Utilization of amylose-lipid complexes as molecular nanocapsules for conjugated linoleic acid. *Biomacromolecules* 6, 121-130.

Le Bail, P., Rondeau, C., Buléon, A., 2005. Structural investigation of amylose complexes with small ligands: helical conformation, crystalline structure and thermostability. *International Journal of Biological Macromolecules* 35, 1-7.

- Lehmann, U., Robin, F., 2007. Slowly digestible starch—its structure and health implications: a review. *Trends in Food Science & Technology* 18, 346-355.
- Lesmes, U., Barchechath, J., Shimoni, E., 2008. Continuous dual feed homogenization for the production of starch inclusion complexes for controlled release of nutrients. *Innovative Food Science & Emerging Technologies* 9, 507-515.
- Lesmes, U., Cohen, S.H., Shener, Y., Shimoni, E., 2009. Effects of long chain fatty acid unsaturation on the structure and controlled release properties of amylose complexes. *Food Hydrocolloids* 23, 667-675.
- Li, W., Peng, H., Ning, F., Yao, L., Luo, M., Zhao, Q., Zhu, X., Xiong, H., 2014a. Amphiphilic chitosan derivative-based core-shell micelles: Synthesis, characterisation and properties for sustained release of Vitamin D₃. *Food chemistry* 152, 307-315.
- Li, W., Peng, H., Ning, F., Yao, L., Luo, M., Zhao, Q., Zhu, X., Xiong, H., 2014b. Amphiphilic chitosan derivative-based core-shell micelles: Synthesis, characterisation and properties for sustained release of Vitamin D₃. *Food chemistry* 152, 307-315.
- Madrigal-Carballo, S., Lim, S., Rodriguez, G., Vila, A.O., Krueger, C.G., Gunasekaran, S., Reed, J.D., 2010. Biopolymer coating of soybean lecithin liposomes via layer-by-layer self-assembly as novel delivery system for ellagic acid. *Journal of Functional Foods* 2, 99-106.
- Mason, T., Paniwnyk, L., Lorimer, J., 1996. The uses of ultrasound in food technology. *Ultrasonics sonochemistry* 3, S253-S260.
- Mason, T.G., Wilking, J., Meleson, K., Chang, C., Graves, S., 2006. Nanoemulsions: formation, structure, and physical properties. *Journal of Physics: Condensed Matter* 18, R635.
- Matalanis, A., Jones, O.G., McClements, D.J., 2011. Structured biopolymer-based delivery systems for encapsulation, protection, and release of lipophilic compounds. *Food Hydrocolloids* 25, 1865-1880.
- Merisko-Liversidge, E.M., Liversidge, G.G., 2008. Drug nanoparticles: formulating poorly water-soluble compounds. *Toxicologic pathology* 36, 43-48.
- Mora-Huertas, C., Fessi, H., Elaissari, A., 2010. Polymer-based nanocapsules for drug delivery. *International journal of pharmaceutics* 385, 113-142.

- Mozafari, M.R., Khosravi-Darani, K., Borazan, G.G., Cui, J., Pardakhty, A., Yurdugul, S., 2008. Encapsulation of food ingredients using nanoliposome technology. *International Journal of Food Properties* 11, 833-844.
- Pettifor, J.M., Prentice, A., 2011. The role of vitamin D in paediatric bone health. *Best Practice & Research Clinical Endocrinology & Metabolism* 25, 573-584.
- Picciano, M.F., 2010. Vitamin D status and health. *Critical reviews in food science and nutrition* 50, 24-25.
- Pittas, A.G., Chung, M., Trikalinos, T., Mitri, J., Brendel, M., Patel, K., Lichtenstein, A.H., Lau, J., Balk, E.M., 2010. Systematic review: Vitamin D and cardiometabolic outcomes. *Annals of internal medicine* 152, 307-314.
- Rajam, R., Karthik, P., Parthasarathi, S., Joseph, G., Anandharamakrishnan, C., 2012. Effect of whey protein-alginate wall systems on survival of microencapsulated *Lactobacillus plantarum* in simulated gastrointestinal conditions. *Journal of Functional Foods* 4, 891-898.
- Raphaelides, S., Karkalas, J., 1988. Thermal dissociation of amylose-fatty acid complexes. *Carbohydrate Research* 172, 65-82.
- Rucker, D., Allan, J.A., Fick, G.H., Hanley, D.A., 2002. Vitamin D insufficiency in a population of healthy western Canadians. *Canadian Medical Association Journal* 166, 1517-1524.
- Shi, A.-M., Wang, L.-J., Li, D., Adhikari, B., 2012. The effect of annealing and cryoprotectants on the properties of vacuum-freeze dried starch nanoparticles. *Carbohydrate Polymers* 88, 1334-1341.
- Shimoni, E., Gustavo, B., 2009. Nanotechnology for foods: Delivery systems. *Global issues in food science and technology* 411, 424.
- Siepmann, J., Siegel, R.A., Rathbone, M.J., 2012. *Fundamentals and applications of controlled release drug delivery*. Springer.
- Simi, C., Abraham, T.E., 2007. Hydrophobic grafted and cross-linked starch nanoparticles for drug delivery. *Bioprocess and biosystems engineering* 30, 173-180.
- Singh, R., Lillard Jr, J.W., 2009. Nanoparticle-based targeted drug delivery. *Experimental and molecular pathology* 86, 215-223.
- Singhvi, G., Singh, M., 2011. Review: in vitro drug release characterization models. *Int J Pharm Stud Res* 2, 77-84.
- Sun, Q., Fan, H., Xiong, L., 2014. Preparation and characterization of starch nanoparticles through ultrasonic-assisted oxidation methods. *Carbohydrate polymers* 106, 359-364.

Tay, S.H., Pang, S.C., Chin, S.F., 2012. A facile approach for controlled synthesis of hydrophilic starch-based

nanoparticles from native sago starch. *Starch-Stärke* 64, 984-990.

Teng, Z., Luo, Y., Wang, Q., 2013a. Carboxymethyl chitosan–soy protein complex nanoparticles for the encapsulation and controlled release of vitamin D₃. *Food chemistry* 141, 524-532.

Teng, Z., Luo, Y., Wang, Q., 2013b. Carboxymethyl chitosan–soy protein complex nanoparticles for the encapsulation and controlled release of vitamin D₃. *Food chemistry* 141, 524-532.

Tischer, P.C.F., Sierakowski, M.R., Westfahl Jr, H., Tischer, C.A., 2010. Nanostructural reorganization of bacterial cellulose by ultrasonic treatment. *Biomacromolecules* 11, 1217-1224.

Tiwari, A., Tiwari, A., 2013. *Bioengineered Nanomaterials*. CRC Press.

Tufvesson, F., Wahlgren, M., Eliasson, A.C., 2003a. Formation of amylose-Lipid complexes and effects of

temperature treatment. Part 1. Monoglycerides. *Starch-Stärke* 55, 61-71.

Tufvesson, F., Wahlgren, M., Eliasson, A.C., 2003b. Formation of Amylose-Lipid Complexes and Effects of

Temperature Treatment. Part 2. Fatty Acids. *Starch-Stärke* 55, 138-149.

Üner, M., 2006. Preparation, characterization and physico-chemical properties of solid lipid nanoparticles (SLN) and nanostructured lipid carriers (NLC): their benefits as colloidal drug carrier systems. *Die Pharmazie-An International Journal of Pharmaceutical Sciences* 61, 375-386.

van Soest, J.J., Tournois, H., de Wit, D., Vliegthart, J.F., 1995. Short-range structure in (partially) crystalline potato starch determined with attenuated total reflectance Fourier-transform IR spectroscopy. *Carbohydrate Research* 279, 201-214.

Zabar, S., Lesmes, U., Katz, I., Shimoni, E., Bianco-Peled, H., 2009. Studying different dimensions of amylose-long chain fatty acid complexes: Molecular, nano and micro level characteristics. *Food Hydrocolloids* 23, 1918-1925.

Zhu, J., Li, L., Chen, L., Li, X., 2012. Study on supramolecular structural changes of ultrasonic treated potato starch granules. *Food Hydrocolloids* 29, 116-122.

Highlight

- Novel high amylose starch based nanoparticles were developed for entrapment of Vitamin D₃.
- Release of encapsulant can be postponed in gastric media.
- Vitamin loaded nanocarriers can be used to produce functional food.

Accepted Manuscript

Table 1. Composition and ultrasonic power in different formulations.

Formulation Code	1	2	3	4	5	6	7	8
Starch concentration (w/w%)	2	2	2	2	4	4	4	4
Ultrasonic power (W)	300	300	450	450	300	300	450	450
Vitamin D ₃ concentration (w/w%)	1.25	2.5	1.25	2.5	1.25	2.5	1.25	2.5

Accepted Manuscript

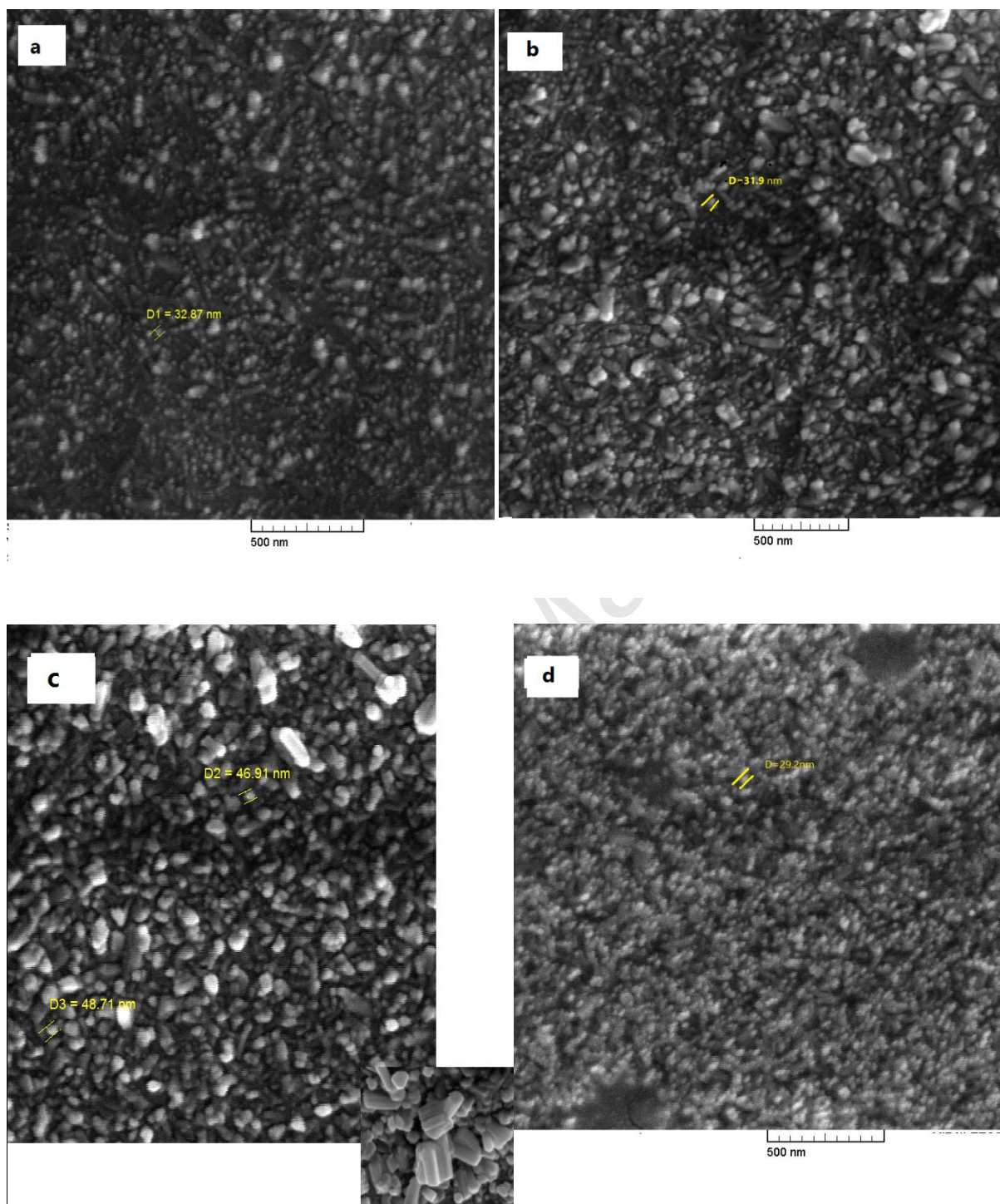
Table 2. Particle size, PDI, zeta potential, encapsulation efficiency, and encapsulation load of developed nanocarriers.

Formulation code	1	2	3	4	5	6	7	8
Size \pm SE (nm)	29.8 \pm 7.71	34.1 \pm 6.35	22.7 \pm 3.2	27.9 \pm 0.66	34 \pm 12.95	39.5 \pm 10.91	14.2 \pm 2.88	31.8 \pm 6.34
PDI \pm SE	0.375 \pm 0.01	0.399 \pm 0.005	0.418 \pm 0.01	0.449 \pm 0.02	0.43 \pm 0.01	0.414 \pm 0.02	0.439 \pm 0.009	0.401 \pm 0.004
Zeta potential \pm SE (mv)	-32.1 \pm 0.53 ^c	-46.05 \pm 0.78 ^a	-37.36 \pm 0.09 ^b	-21.7 \pm 0.02 ^e	-22.67 \pm 0.26 ^e	-29.8 \pm 0.33 ^d	-28.87 \pm 0.46 ^d	-9.81 \pm 0.36 ^f
EE \pm SE (%)	48.3 \pm 0.96 ^b	55.94 \pm 2.94 ^c	78.11 \pm 0.97 ^d	37.06 \pm 1.64 ^a	38.82 \pm 4.5 ^a	56.45 \pm 2.25 ^c	56.68 \pm 0.15 ^c	71.93 \pm 1.51 ^d
LE \pm SE (%)	0.7 \pm 0.06 ^{ab}	0.93 \pm 0.17 ^{bc}	1.15 \pm 0.07 ^{cd}	0.61 \pm 0.036 ^a	0.46 \pm 0.045 ^a	1.22 \pm 0.08 ^d	0.67 \pm 0.017 ^{ab}	1.55 \pm 0.08 ^e

Different letters show significant differences in 95% confidence

Table 3. Model parameters of vitamin D₃ release.

Hixson Crowen		Quadratic			Wibull		Baker Lonsdale			Rigter–Peppas			Higuchi		Fist order		Zero order		Formulatio n	Release condition
R	K	R	k2	k1	R	b	a	R	k	R	n	K	R	K	R	K	R	k		
0.976	2.623	0.982	0.0398	0.012	0.97	0.692	0.93	0.344	1.381	0.965	0.45	0.588	0.97	2.518	0.77	0.733	0.689	2.03	1	Gastric
0.942	3.053	0.872	0.0548	0.0197	0.926	0.493	1.99	0.339	1.38	0.903	0.183	0.85	0.8	2.9	0.12	0.824	0.156	2.29	2	
0.76	0.535	0.935	0.00491	0.00032	0.844	1.66	0.04	0.147	1.196	0.841	1.36	0.07	0.86	0.522	0.609	0.371	0.932	0.439	3	
0.796	2.69	0.649	0.05	0.0192	0.786	0.265	3.5	0.348	1.385	0.905	0.027	0.966	0.796	2.735	0.268	0.72	0.268	1.97	4	
0.429	1.035	0.938	0.00205	0.00705	0.514	1.067	0.89	0.306	25.72	0.974	2.167	1.556	0.545	1.03	0.24	0.059	0.78	0.933	5	
0.883	0.467	0.781	0.00863	0.0032	0.923	0.4	2.51	0.347	1.384	0.901	0.103	0.914	0.69	0.442	0.73	48.09	0.054	0.346	6	
0.908	2.187	0.73	0.03805	0.0134	0.911	0.419	2.14	0.345	1.384	0.943	0.132	0.872	0.746	2.07	0.15	0.589	0.065	1.63	7	
0.876	0.856	0.737	0.01562	0.00574	0.936	0.376	2.46	0.348	1.385	0.956	0.095	0.906	0.688	0.81	0.94	0.059	0.066	0.634	8	
0.951	41.17	0.966	0.2665	0.0225	0.883	0.325	2.58	0.564	0.87	0.876	0.08	14.295	0.87	30.58	0.413	0.709	0.481	12.08	1	Intestinal
0.964	20.74	0.966	0.1308	0.01078	0.924	0.071	1.93	0.812	0.253	0.881	0.116	8.134	0.89	15.42	0.429	0.597	0.529	6.1	2	
0.985	33.86	0.977	0.201	0.0156	0.867	0.11	1.87	0.924	0.32	0.875	0.22	7.272	0.94	25.22	0.453	0.679	0.641	10.03	3	
0.934	30.45	0.949	0.2	0.01723	0.611	0.224	1.88	0.758	0.999	0.843	0.033	17.35	0.847	22.6	0.396	0.66	0.429	8.91	4	
0.992	35.54	0.98	0.208	0.0159	0.971	0.045	4.78	0.691	24.75	0.978	0.237	133.15	0.952	26.47	0.46	0.687	0.661	10.54	5	
0.979	16.944	0.956	0.102	0.00803	0.939	0.047	3.68	0.647	5.5	0.899	0.163	42.588	0.924	12.6	0.45	0.564	0.586	5	6	
0.99	40.065	0.98	0.2364	0.0181	0.945	0.072	2.84	0.763	1.993	0.972	0.228	18.06	0.949	29.83	0.454	0.707	0.653	11.87	7	
0.981	14.782	0.962	0.088	0.00698	0.968	0.057	2.93	0.702	1.96	0.955	0.173	19.73	0.928	11	0.451	0.541	0.604	4.37	8	
0.5	31.19	0.799	0.163	0.007	0.942	0.626	0.95	0.589	0.762	0.826	1.58	0.843	0.65	25.685	0.721	0.711	0.773	11.6	1	Whole release process
0.539	16.16	0.832	0.0867	0.0044	0.362	0.141	1.85	0.157	0.174	0.796	1.138	1.133	0.69	13.236	0.566	0.608	0.793	5.92	2	
0.489	25.24	0.815	0.117	0.0034	0.91	2.109	0.05	0.335	0.247	0.883	2.523	0.107	0.64	20.9	0.679	0.628	0.807	9.57	3	
0.5	23.26	0.792	0.1259	0.00643	0.053	-	3.2	0.637	0.884	0.749	1.322	1.419	0.65	19.1	0.639	0.663	0.757	8.58	4	
0.498	26.61	0.827	0.123	0.00365	0.789	1.01	0.94	0.597	22.52	0.935	2.615	2.022	0.657	22.03	0.667	0.651	0.819	10.07	5	
0.491	12.67	0.807	0.0601	0.00198	0.901	0.283	2.52	0.78	5.17	0.764	1.867	1.536	0.646	10.48	0.67	0.513	0.797	4.78	6	
0.506	30.262	0.829	0.1432	0.00471	0.871	0.269	2.1	0.746	1.83	0.778	1.562	1.325	0.665	24.99	0.743	0.701	0.819	11.38	7	
0.504	11.178	0.818	0.054	0.00195	0.795	0.2	3.78	0.783	1.8	0.769	1.533	1.381	0.66	9.22	0.74	0.512	0.805	4.19	8	



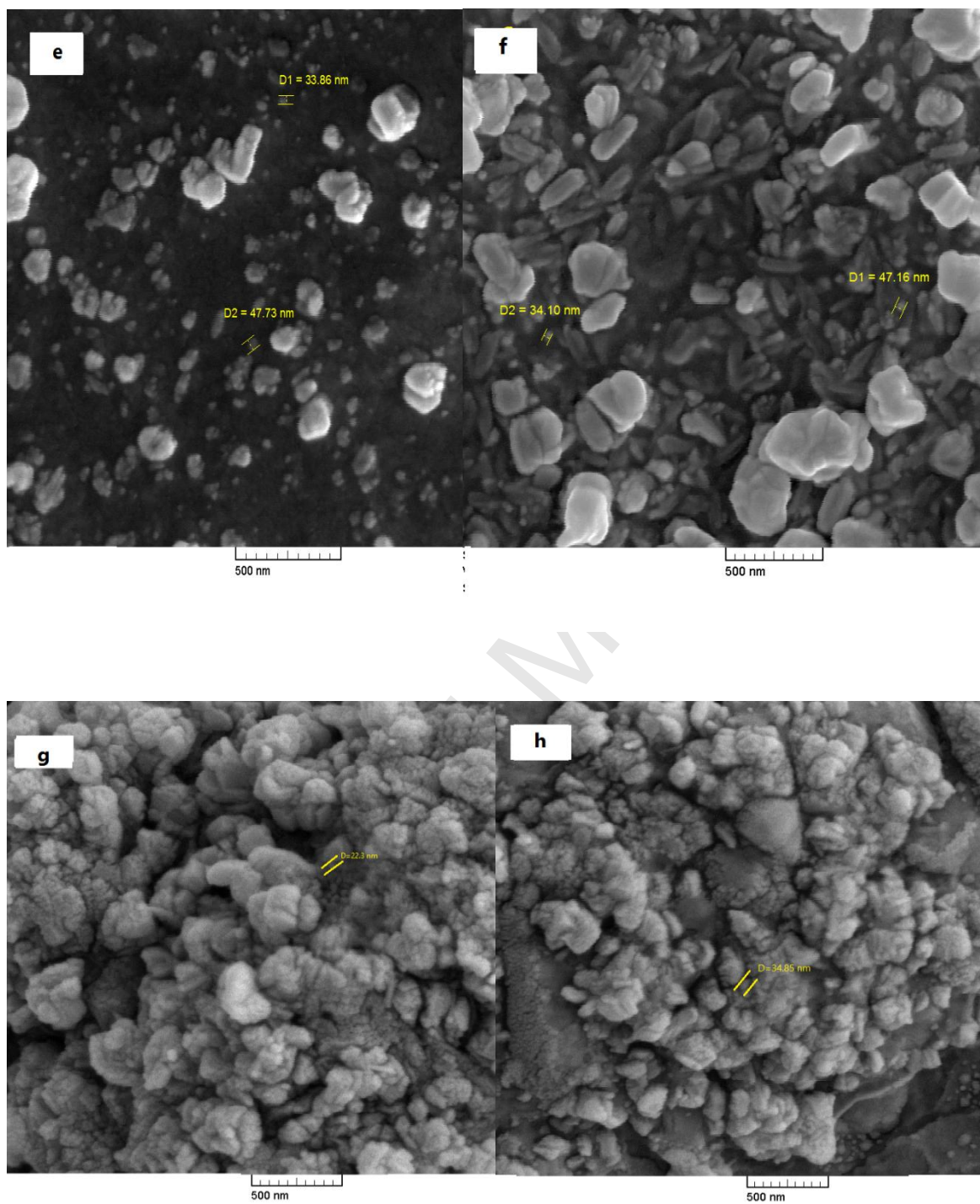
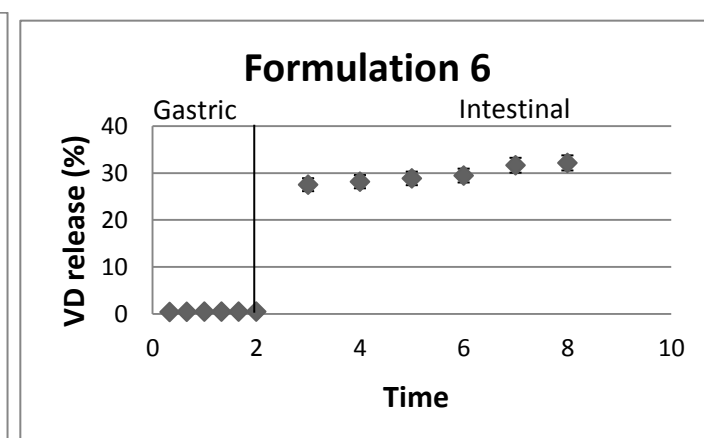
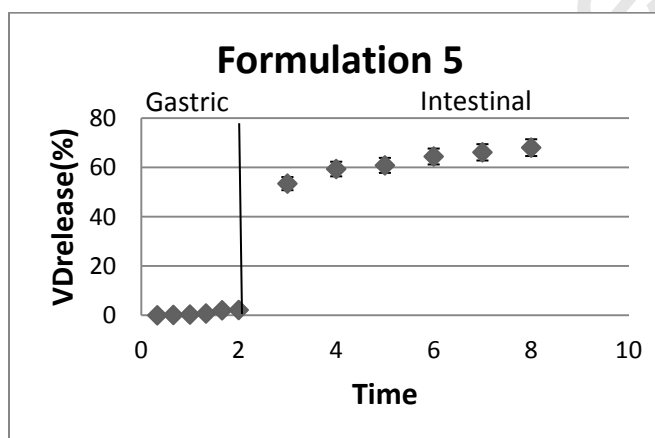
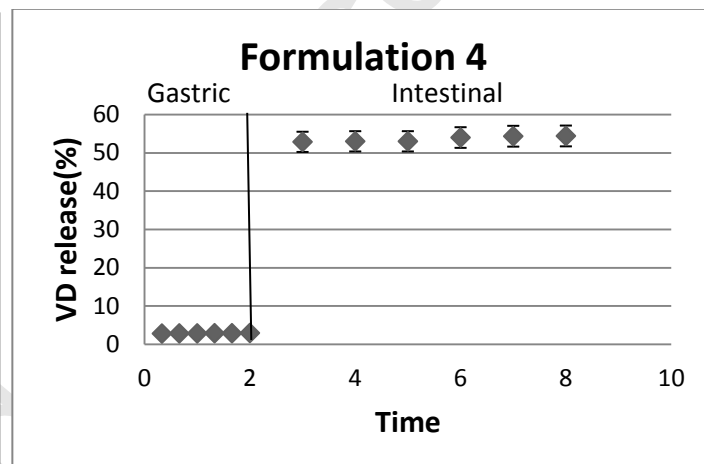
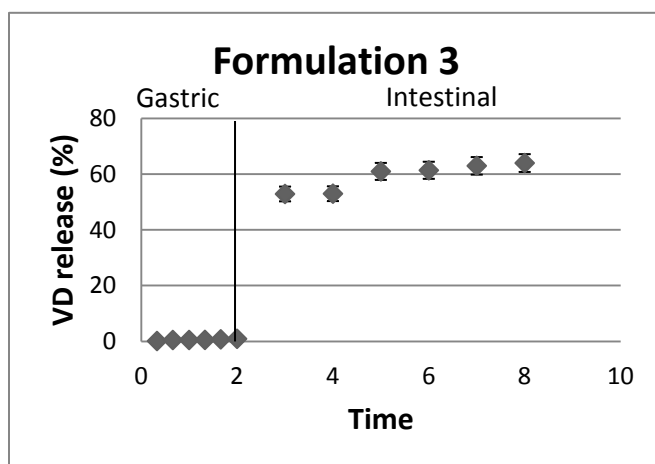
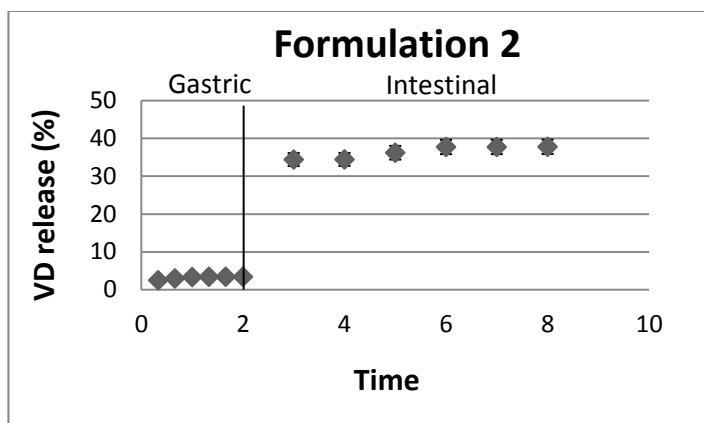
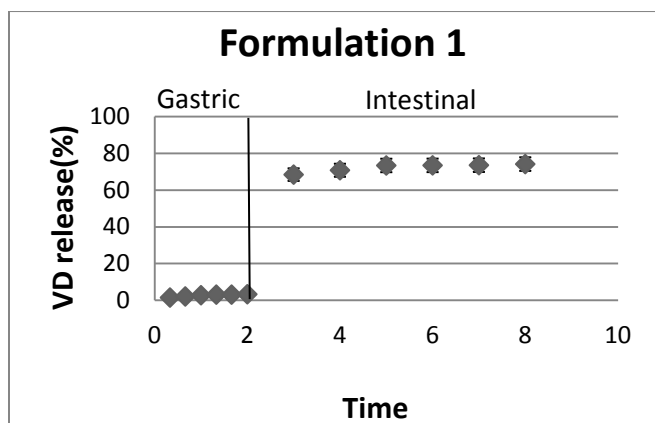


Fig.1. SEM images of VD-loaded nanoparticles: (a) formulation 1, (b) formulation 2, (c) formulation 3, (d) formulation 4, (e) formulation 5, (f) formulation 6, (g) formulation 7, (h) formulation 8.



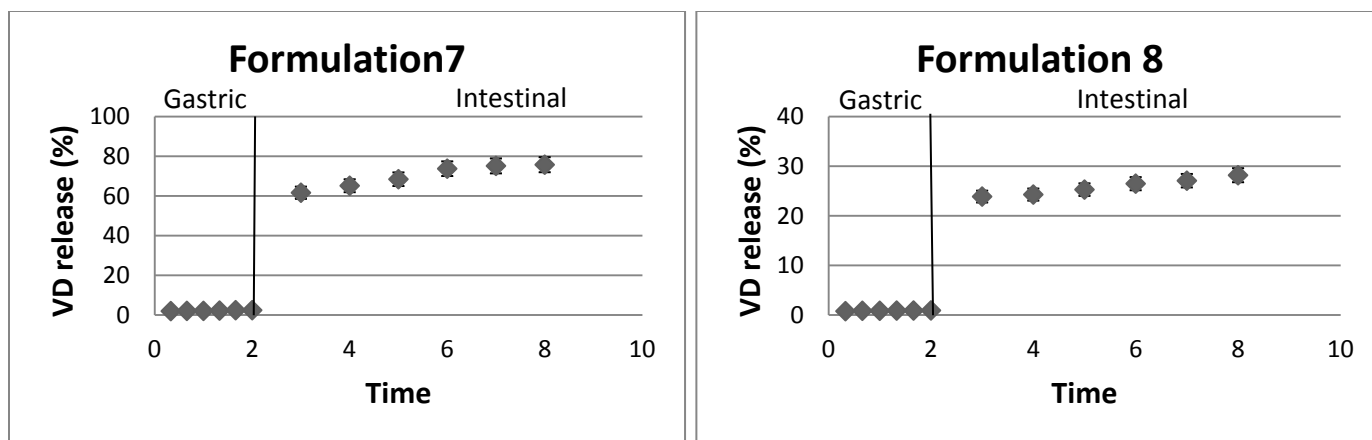
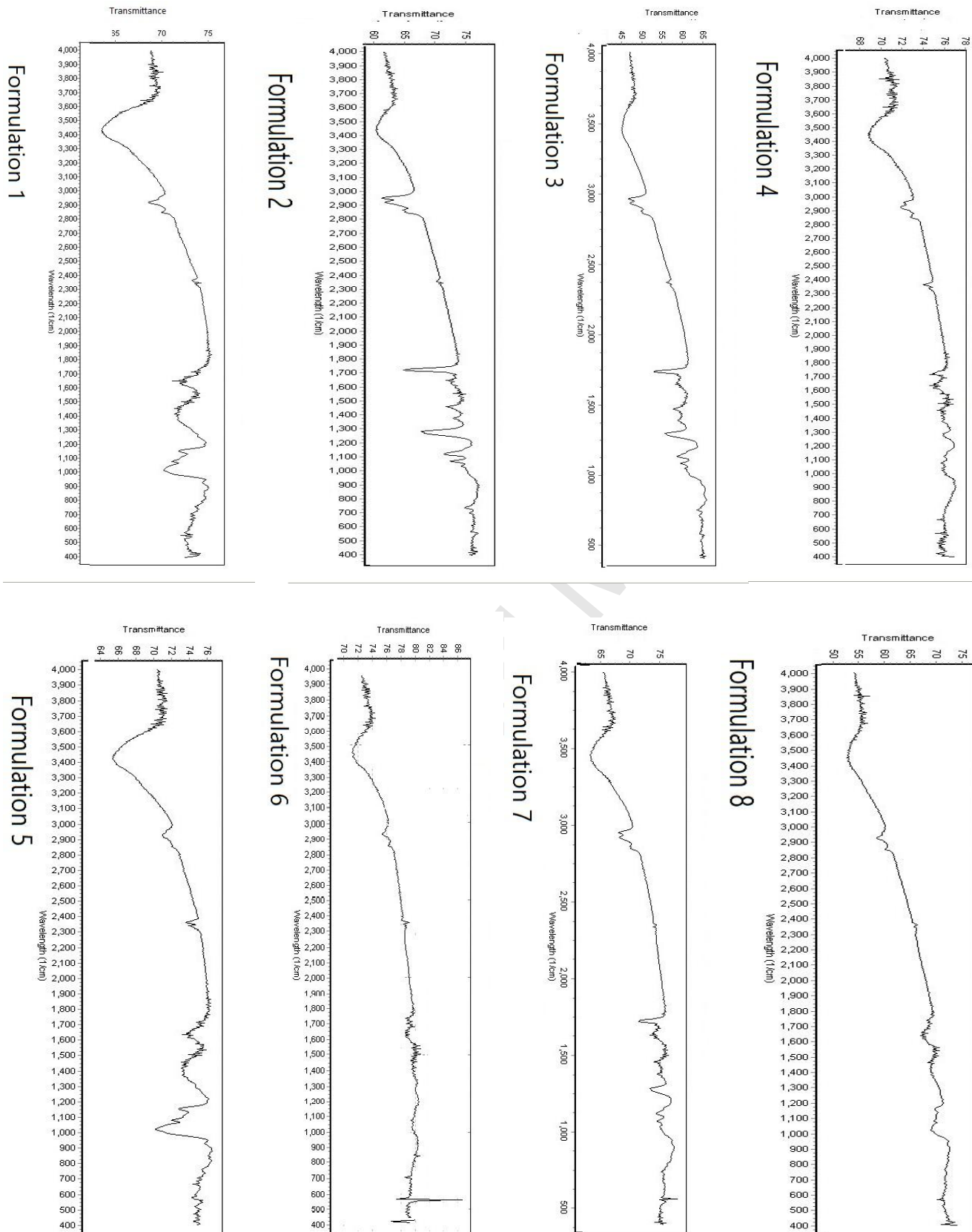


Fig. 2. Release profile of vitamin D₃ from different developed nanocarriers.



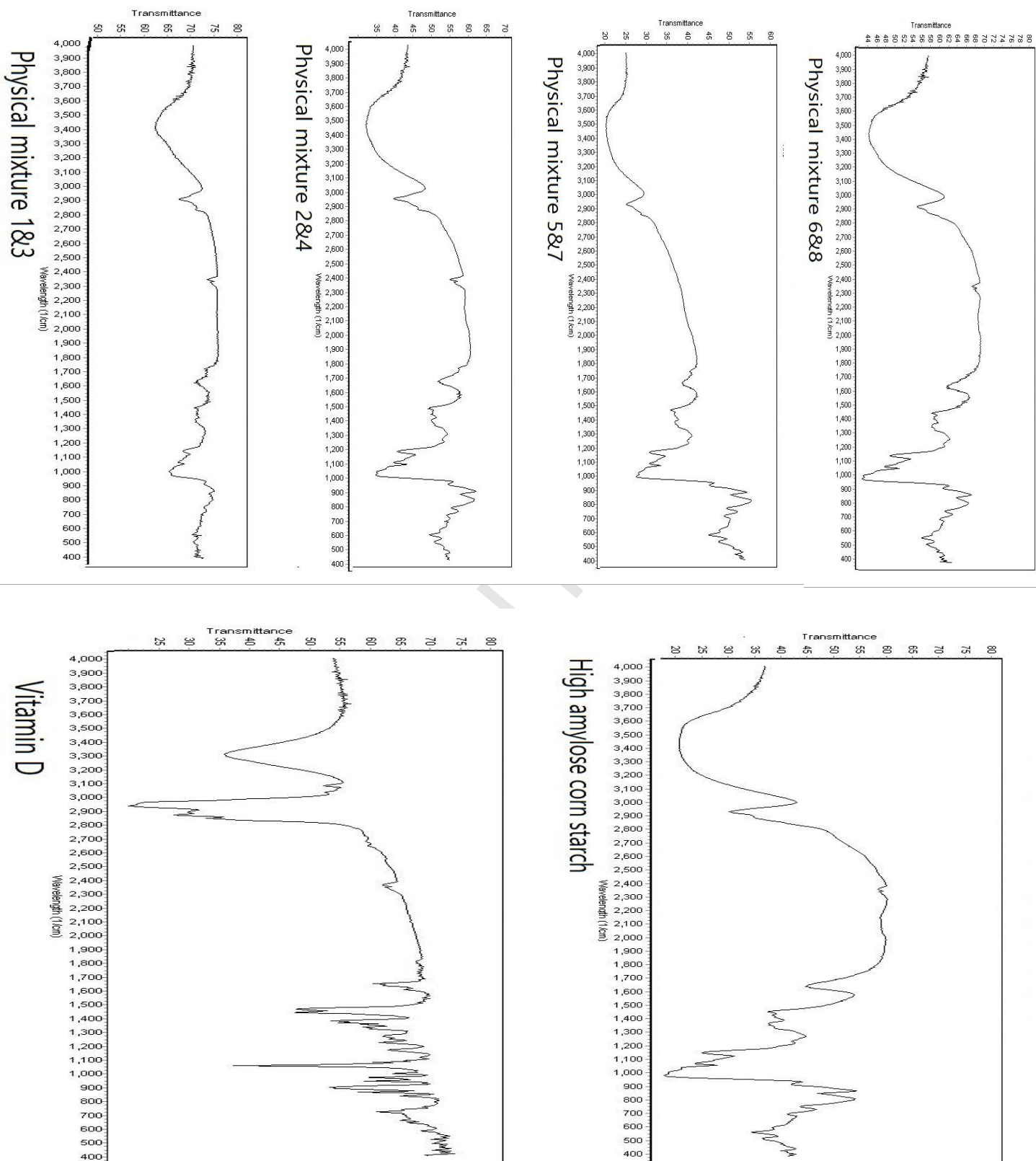
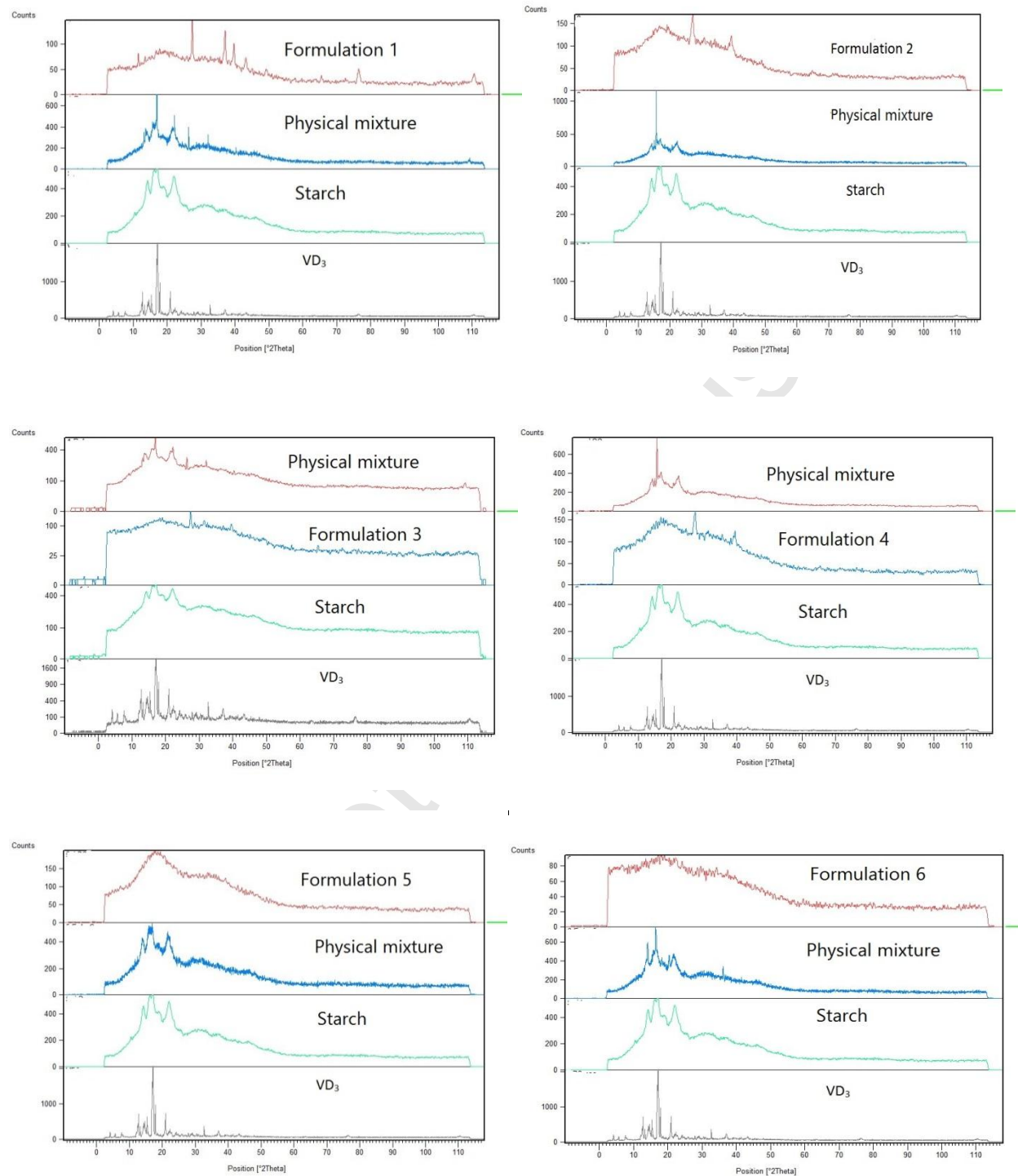


Fig. 3. FTIR spectrum of pure materials and different developed nanoparticles.



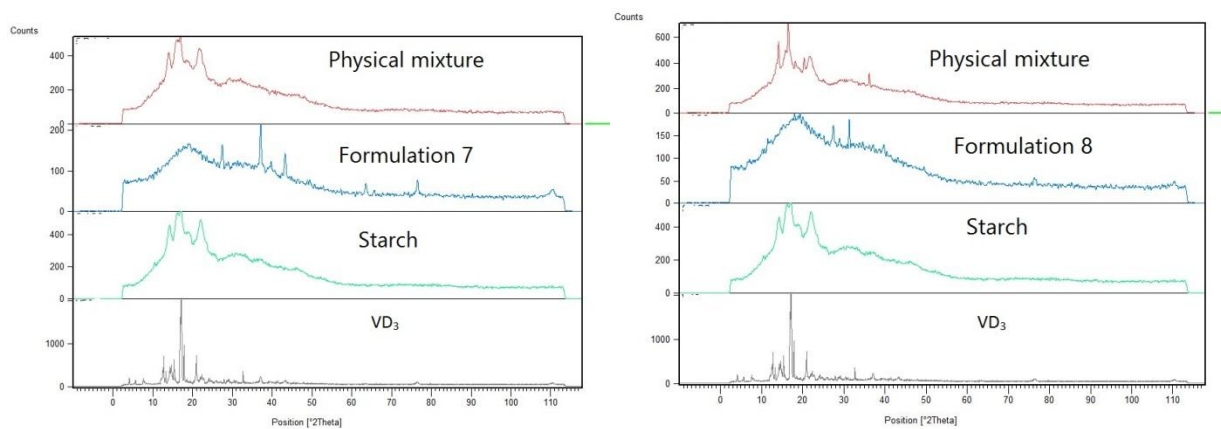
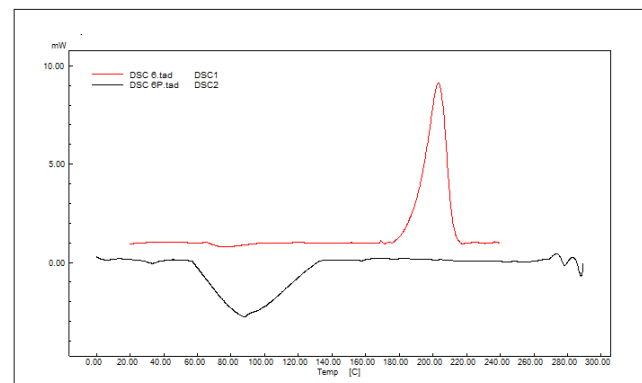
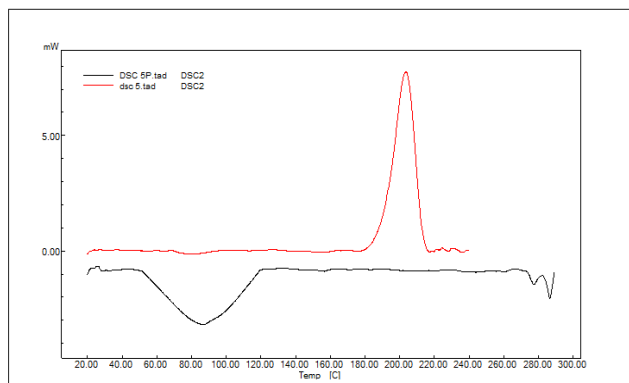
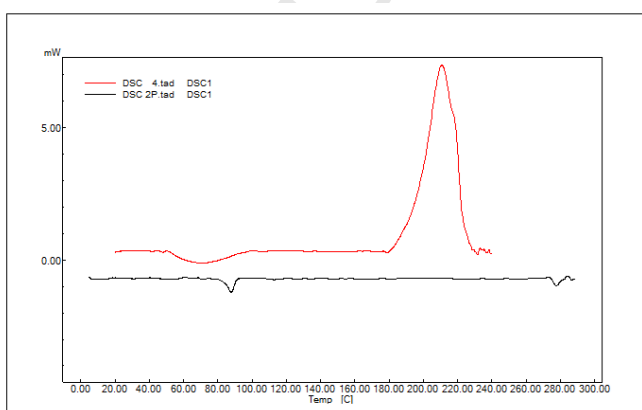
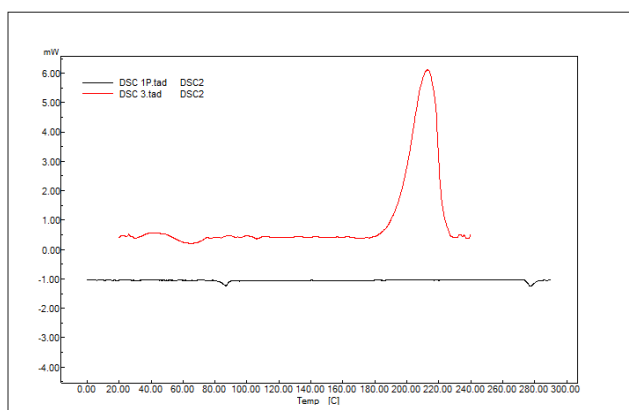
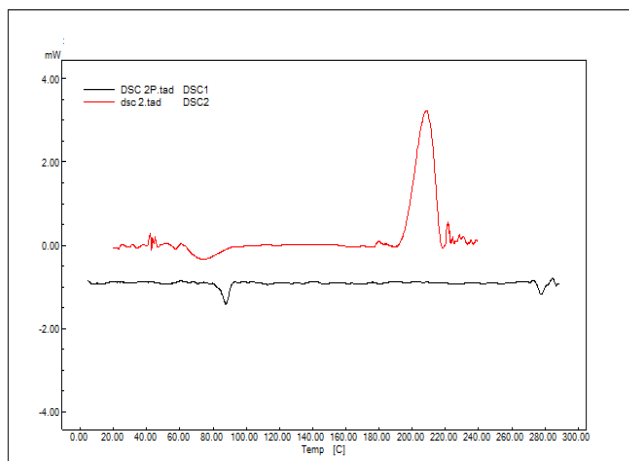
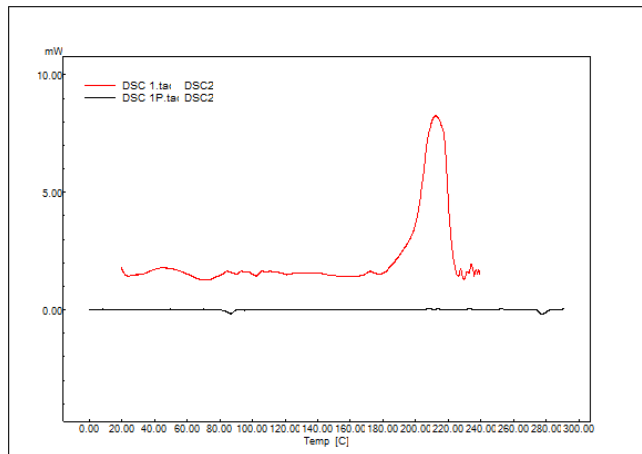


Fig.4. Comparison of diffractograms of pure materials with different developed nanocarriers and physical mixture of starch and vitamin D.



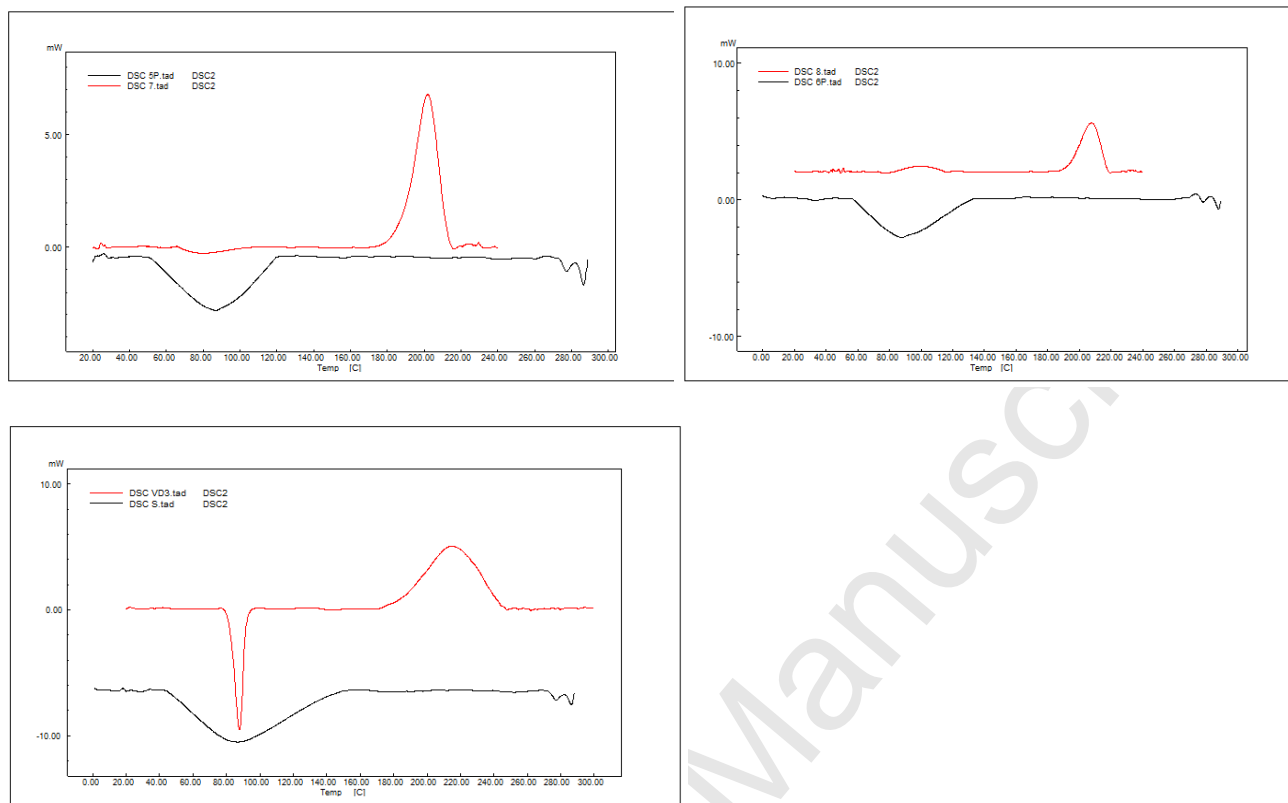


Fig.5. Comparison of curves DSC of nanoparticles with physical mixture of starch and vitamin D.

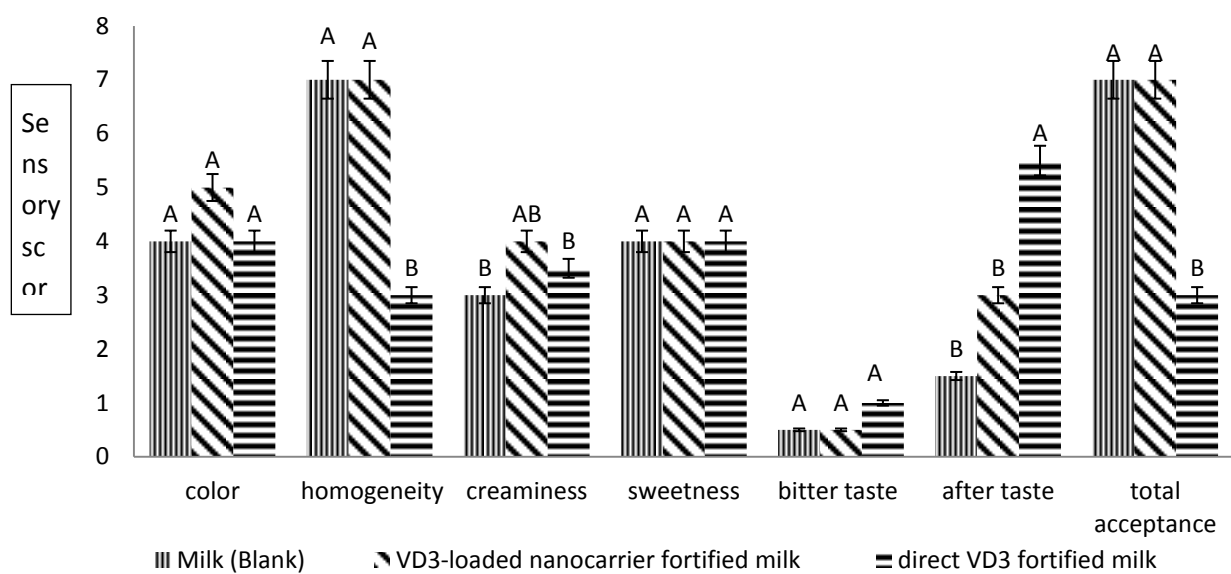


Fig .6. Sensory results of fortified milk (different letters for each sensory feature indicating statistically significant differences; $p < 0.05$)